Available online at www.sciencedirect.com
SCIENCE DIRECT
Dyes and Pigments 70 (2006) 171–176
DYES and PIGMENTS
www.elsevier.com/locate/dyepig

Writing–erasing properties and characterizations of hybrid materials based on disperse red by sol–gel process

Mi-Ra Kim [a,*], Young-Il Choi [b], Sang-Wook Park [c], Jae-Wook Lee [d], Jin-Kook Lee [b]

[a] Center for Plastic Information System, Pusan National University, Busan 609-735, Korea
[b] Department of Polymer Science & Engineering, Pusan National University, Busan 609-735, Korea
[c] Department of Chemical Engineering, Pusan National University, Busan 609-735, Korea
[d] Division of Chemical Engineering, Sogang University, Seoul 121-742, Korea

Received 21 November 2004; accepted 15 April 2005
Available online 20 July 2005

Abstract

We investigated the synthesis and writing–erasing properties of three different hybrid materials (SGDR1, SGDR13 and SGDR19) based on disperse red by the sol–gel process. The sol–gel process was undergone using tetraethyl orthosilicate (TEOS) as a precursor. Optical properties of three hybrid materials are compared as structurally similar materials (SGDR1, SGDR13 and SGDR19). The diffraction efficiency, reversible photoinduced process and writing–erasing properties of hybrid materials were measured as a function of time. The diffraction efficiencies of SGDR1, SGDR13, and SGDR19 films were observed up to a level of 0.65%, 0.24%, and 0.99%, respectively. AFM view of the surface relief grating on the SGDR19 film showed a depth of 15 nm and a surface distance of 2.50 μm.

Keywords: Sol–gel process; Disperse red; Diffraction efficiency; Writing–erasing properties; Surface relief grating

1. Introduction

The materials containing an azobenzene unit are generally used for the writing records and in reading and erasing steps. Until recently, the materials have been made from organic polymers such as host passive matrices where the active dye molecules as methyl orange, methyl red, or disperse red 1 were introduced as guest materials. These materials were casted on various substrates to provide thin films in which the doping molecules are either dispersed into [1,2] or grafted onto [3,4] the polymer backbone. Also, organic–inorganic hybrid materials containing azobenzene unit by the sol–gel process have been studied in the field of optical data storage, nonlinear optical, and holographic applications [5–11]. The sol–gel process involving hydrolysis and condensation can form various microstructures as a matrix with the high optical quality at low temperature. The large variety of suitable organic molecules allows a controlling of optical, chemical and mechanical properties [12]. For optical information storage and erasing, as known, optically induced anisotropy in the azobenzene containing material is required. When the film is irradiated with a linearly polarized laser beam, the photochemically induced *trans–cis* photoisomerization of the azobenzene group within film can generate photoinduced birefringence through the reorientation of azobenzene molecules.

We synthesized the Organically Modified Silanes (ORMOSILs) containing disperse red 19 (DR19),

* Corresponding author. Tel.: +82 51 510 3045; fax: +82 51 513 7720.
E-mail address: mrkim2@pusan.ac.kr (M.-R. Kim).

0143-7208/$ - see front matter © 2005 Elsevier Ltd. All rights reserved.
doi:10.1016/j.dyepig.2005.04.018

disperse red 13 (DR13), or disperse red 1 (DR1) as optical data storage materials. The sol–gel process was undergone using tetraethyl orthosilicate (TEOS) as precursors. The diffraction efficiencies of hybrid materials (SGDR1, SGDR13 and SGDR19) obtained by the sol–gel process were measured as a function of time.

2. Experimental

2.1. Materials

Disperse Red 1 (DR1), Disperse Red 13 (DR13), Disperse Red 19 (DR19), 3-(triethoxysilyl)propyl isocyanate (ICPTEOS), tetraethylortho silicate (TEOS), obtained from Aldrich Co., were used without further purification. *N*,*N*′-dimethylformamide (DMF), tetrahydrofuran (THF), dimethyl sulfoxide (DMSO), *n*-hexane and chloroform were used as received from Aldrich Co. Other chemicals were of reagent grade and were used without further purification.

2.2. Characterization

FT-IR spectra were recorded using a JASCO 460 spectrophotometer. ^{1}H NMR spectra were recorded using a Varian Unity Plus 300 (300 MHz) spectrophotometer using tetramethylsilane (TMS) as an internal standard. UV–visible spectra were recorded using a UVIKON 860 spectrophotometer.

2.3. Syntheses of DR-n-Ts/SGDR-ns and preparations of films

The structurally similar DR1T, DR13T and DR19T containing different azobenzene groups were prepared. Typical synthesis of DR1T was carried out as follows. A solution of DR1 (0.4 g, 1.272 mmol) and 3-(triethoxysilyl) propyl isocyanate (ICPTEOS) (0.315 g, 1.272 mmol) in tetrahydrofuran (THF) (10 mL) was heated to 70 °C with vigorous stirring under nitrogen purge for 24 h. The reaction mixture was cooled to room temperature, and then poured into *n*-hexane. The resulting precipitates were reprecipitated into *n*-hexane and dried in a vacuum oven for 24 h. The product (DR1T) was obtained as a dark red powder. For the syntheses of DR13T or DR19T, the same procedures were followed as described above except that for DR13 (0.4 g, 1.147 mmol)/3-(triethoxysilyl)propyl isocyanate (ICPTEOS) (0.2837 g, 1.147 mmol) or DR19 (0.4 g, 1.211 mmol)/3-(triethoxysilyl)propyl isocyanate (ICPTEOS) (0.6 g, 2.422 mmol) replaced DR1 (0.4 g, 1.272 mmol) and ICPTEOS (0.3 g, 1.272 mmol), respectively. The reaction routes of DR-*n*-Ts are illustrated in Fig. 1.

The products (DR1T, DR13T and DR19T) were dissolved in DMF and each solution was mixed with tetraethyl orthosilicate (TEOS) at room temperature for 10 min. Then, the mixture of water and HC1 was added drop-wise for 30 min. The solution was hydrolyzed and condensed at room temperature for 90 min. The total molar ratios of reactions are summarized in Table 1.

For studying the optical properties, we fabricated a thin film. The sol was filtered with a 0.2 μm nylon filter and spin-coated onto a clean slide glass with 1000 rpm. And coated glasses were dried in a vacuum oven at 80 °C for 2 h. The thickness of the films, measured using a Dektak3 (Alpha-step), were about 1.28 μm, 1.62 μm and 1.37 μm. for SGDR1, SGDR13, and SGDR19, respectively.

2.4. Experimental setup and real-time dynamic holographic recording

The schematic diagram of the experimental setup is shown in Fig. 2. A linearly polarized Ar^+ laser of 488 nm was used as the pump beam and an He–Ne laser beam at 633 nm as the probe beam. The intensity of the probe beam was set to 1.0 mW/cm^2. Real-time holographic recording was performed by employing two recording beams at 488 nm from an Ar^+ laser. The interbeam angle was set to 11° in all of the experiments. The reading beam was set at 633 nm from an He–Ne laser. The continuous dynamic reading of the diffraction light with a photometer allowed synchronous observation of the diffraction efficiency. The diffraction efficiency (η) is defined as

$$\eta = I_d / I_i \quad (1)$$

where I_d is the intensity of the first order diffracted beam and I_i is the intensity of input beam.

3. Results and discussion

SGDR-*n*s containing azobenzene groups were synthesized by the sol–gel process of TEOS and their precursors (DR-*n*-Ts). The chemical structures of DR-*n*-Ts are shown in Fig. 1. The structures of synthesized DR-*n*-Ts were confirmed by FT-IR and ^{1}H NMR spectroscopy. In Fig. 3, the FT-IR spectra of DR-*n*-Ts showed characteristic absorption peaks at 1706–1694 cm^{-1} due to C=O stretching of the urethane group, at 1251–1245 cm^{-1} due to C–N and C–O coupled stretching of the urethane group, and at 1080–1078 cm^{-1} and 957–956 cm^{-1} due to Si–O–C asym and sym stretching of the ICPTEOS, respectively. The ^{1}H NMR spectrum of DR19T exhibited characteristic peaks at δ 7.09 ppm assignable to the N–H of the urethane linkage, δ 8.25–6.80 ppm assignable to aromatic group of the azobenzene and δ 3.62–0.35 ppm assignable to aliphatic group of the ICPTEOS. The UV–vis absorption spectra of SGDR-*n*s are shown in Fig. 4. The absorption spectra of SGDR-*n*s had maximums of

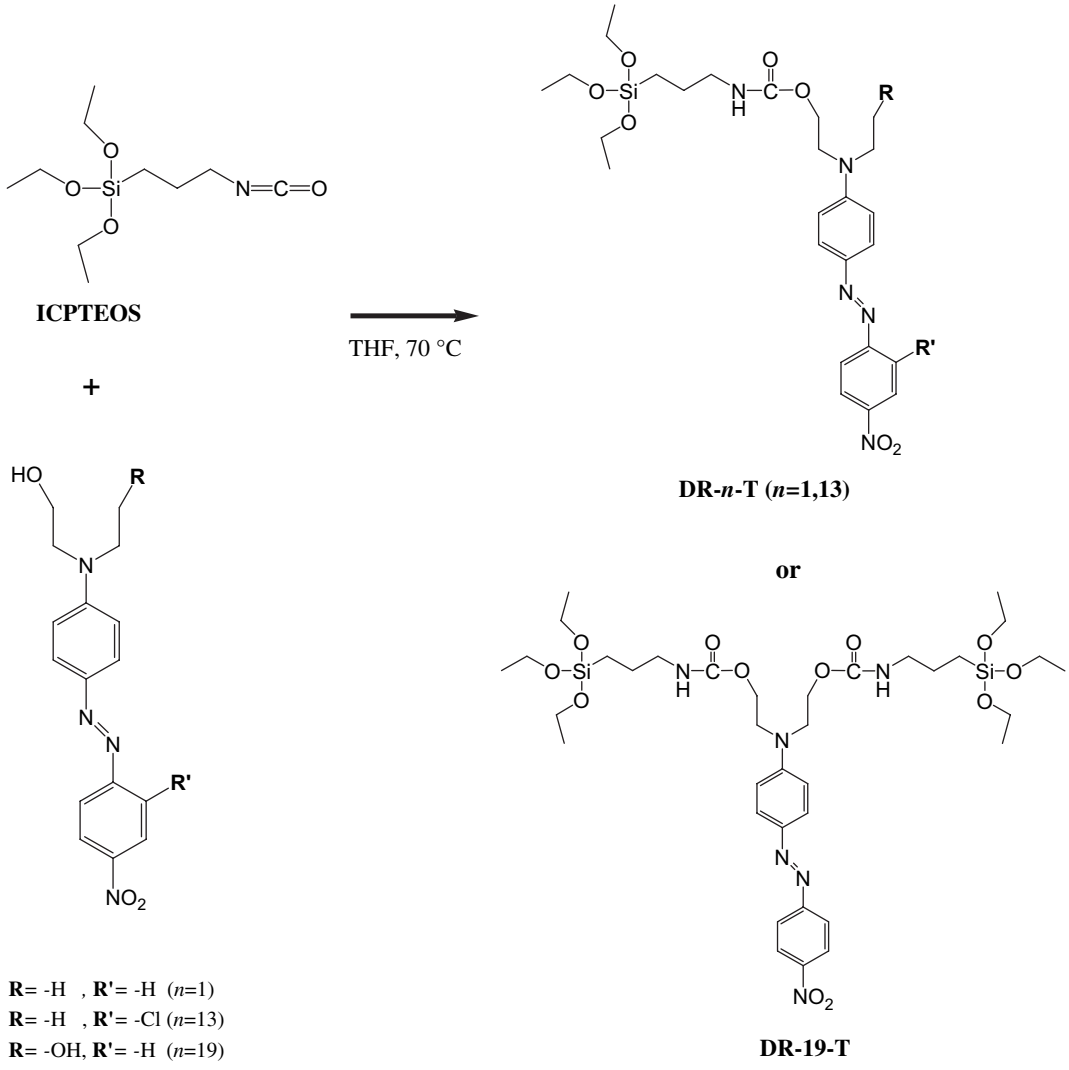

Fig. 1. The synthetic routes and the structures of DR-*n*-Ts.

427, 466, and 441 nm. The characterizations of DR-*n*-Ts as the structures were as follows.

3.1. Spectral data for DR1T

FT-IR (THF solution, cm^{-1}), 3334 (NH stretching), 1694 (C=O stretching), 1516 (NO_2 asym stretching), 1388 (NO_2 sym stretching), 1251 (C–N and C–O coupled stretching), 1080 (Si–O–C asym stretching), 956 (Si–O–C sym stretching); ^{1}H NMR (DMSO–d_6, ppm), δ 8.24–8.21, 7.81–7.78 (4H, NO_2-aromatic-N=N–), 7.72–7.69, 6.79–6.76 (4H, –N=N-aromatic-N–), 7.09 (1H, –NH–), 4.01 (2H, $-NCH_2CH_2O-$), 3.62–3.51 (6H, $-Si-OCH_2CH_3$), 3.44–3.36 (2H, $-NCH_2CH_2O-$), 3.44–3.36 (2H, $-NCH_2CH_3$), 2.82–2.80 (2H, $-Si-CH_2CH_2CH_2N-$), 1.31–1.25 (2H, $-Si-CH_2CH_2CH_2N-$), 1.05–0.95 (9H, $-Si-OCH_2CH_3$), 0.96–0.90 (3H, $-NCH_2CH_3$), 0.40–0.35 (2H, $-Si-CH_2CH_2CH_2N-$).

3.2. Spectral data for DR13T

FT-IR (THF solution): NH stretching 3351 cm^{-1}, C=O stretching 1705 cm^{-1}, C–N and C–O coupled stretching 1238 cm^{-1}, Si–O–C stretching 1077 cm^{-1} (asym) 958 cm^{-1} (sym), NO_2 stretching 1517 cm^{-1} (asym) 1374 cm^{-1} (sym); ^{1}H NMR (DMSO–d_6, ppm):

Table 1
Molar ratio of sol solution of SGDR-*n*s for the sol–gel process

	Disperse Red	ICPTEOS[a]	TEOS[b]	H_2O	HC1	DMF[c]
SGDR1	1[d]	1	3	16	0.104	32
SGDR13	1[e]	1	3	16	0.104	32
SGDR19	1[f]	2	2	16	0.104	32

[a] 3-(Triethoxysilyl)propyl isocyanate.
[b] Tetraethyl orthosilicate.
[c] *N*,*N*′-dimethylformamide.
[d] Disperse Red 1.
[e] Disperse Red 13.
[f] Disperse Red 19.

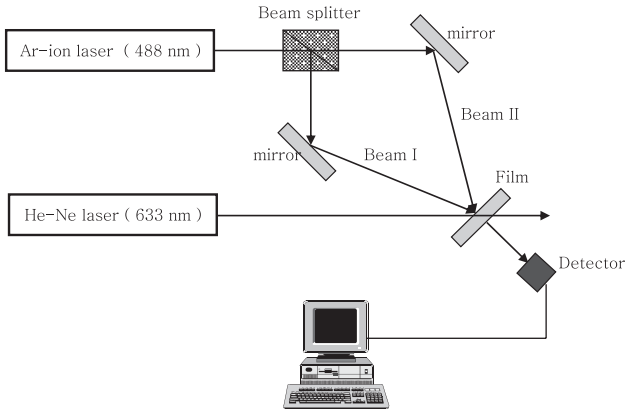

Fig. 2. Experimental setup used to measure diffraction efficiency.

δ 8.30–8.29, 8.13–8.10, 7.73–7.70 (3H, NO_2-aromatic-N=N–), 7.67–7.64, 6.81–6.76 (4H, –N=N-aromatic-N–), 7.10 (1H, –NH–), 3.44–3.36 (2H, –NCH_2CH$_2$O–), 4.02 (2H, –NCH$_2$CH_2O–), 3.44–3.36 (2H, –NCH_2CH$_3$), 0.96–0.92 (3H, –NCH$_2$CH_3), 3.63–3.55 (6H, –Si–OCH_2CH$_3$), 1.05–0.95 (9H, –Si–OCH$_2$CH_3), 0.40–0.35 (2H, –Si–CH_2CH$_2$CH$_2$N–), 1.31–1.25 (2H, –Si–CH$_2$CH_2CH$_2$N–), 2.81–2.79 (2H, –Si–CH$_2$CH$_2$CH_2N–).

3.3. Spectral data for DR19T

FT-IR (THF solution, cm^{-1}), 3335 (NH stretching), 1706 (C=O stretching), 1517 (NO_2 asym stretching), 1386 (NO_2 sym stretching), 1245 (C–N and C–O coupled stretching), 1078 (Si–O–C asym stretching), 957 (Si–O–C sym stretching); ^{1}H NMR (DMSO–d_6, ppm), δ 8.25–8.22, 7.82–7.80 (4H, NO_2-aromatic-N=N–), 7.70–7.68, 6.85–6.80 (4H, –N=N-aromatic-N–), 7.09 (2H, –NH–), 4.02 (4H, –NCH$_2$CH_2O–), 3.62–3.55 (12H, –Si–OCH_2CH$_3$), 3.43–3.40 (4H, –NCH_2CH$_2$O–), 2.81–2.79 (4H, –Si–CH$_2$CH$_2$CH_2N–), 1.31–1.25 (4H, –Si–CH$_2$CH_2CH$_2$N–), 1.01–0.95 (18H, –Si–OCH$_2$CH_3), 0.40–0.35 (4H, –Si–CH_2CH$_2$CH$_2$N–).

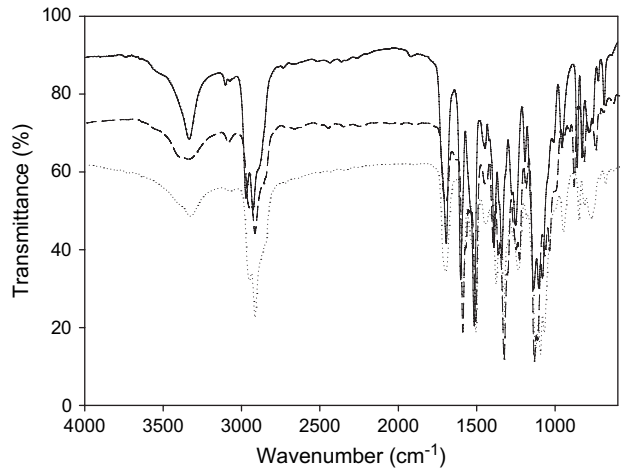

Fig. 3. FT-IR spectra of SGDR1 (solid line), SGDR13 (dashed line) and SGDR19 (dotted line) films.

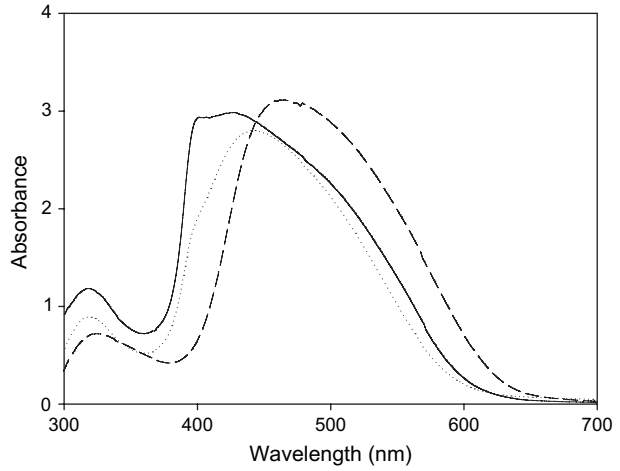

Fig 4. UV–vis absorption spectra of SGDR1 (solid line), SGDR13 (dashed line) and SGDR19 (dotted line) films.

Fig. 5 shows the diffraction efficiency as a function of time for SGDR-*n*s during the recording process. An Ar^+ laser beam at 488 nm with an intensity of 25 mW/cm^2 was used. As the orientation grating was formed, the diffraction efficiency increased, saturated, and remained at a constant value throughout the rest of the recording process. When the writing beam was turned on, the diffraction efficiency increased rapidly and reached 0.65%, 0.24% and 0.99% in SGDR1, SGDR13 and SGDR19, respectively. After the one beam was turned off, the diffraction efficiency decayed to nearly zero, indicating that most of the orientation grating had been erased.

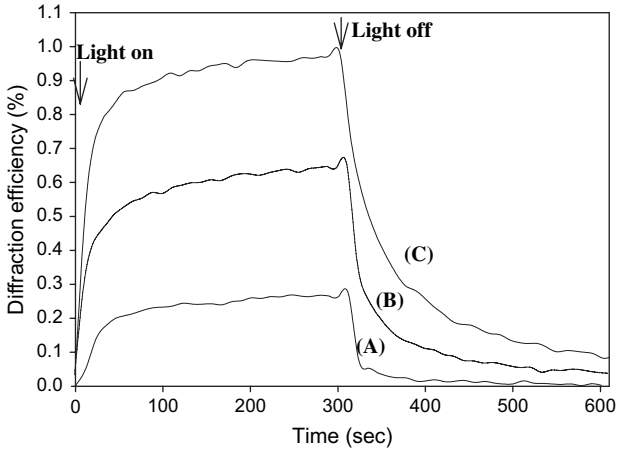

Fig. 5. Diffraction efficiency as a function of time for SGDR1 (B), SGDR13 (A), and SGDR19 (C) under the polarization recording condition with an intensity of 25 mW/cm^2.

Fig. 6 gives a typical first write–erase and second write–erase profile of optically induced diffraction efficiency for the SGDR1, SGDR13, and SGDR19. At point A, the linearly polarized two writing beams were turned on and the diffraction efficiency increased. The two writing beams were turned off at point B, and the relaxation occurred to a stable level at point C. When one beam was turned on, erasing was started at point C. Second writing–erasing was also performed as the same manner. At point D, two writing beams were turned on, and one beam was turned off at point E. From this result, we know that the second writing rate is faster than the first one; however, in case of erasing second one is slower than first one.

Surface relief grating with large surface modulations could be formed on the hybrid material with azobenzene group. Fig. 7 shows a typical atomic force microscopic (AFM, Nanoscope III A, Digital Instrument Co.) view of the surface relief gratings formed on SGDR19 film. The gratings were fabricated using simple interference of the two linearly polarized 488 nm beams from an Ar^+ laser with an intensity of 25 mW/cm^2 as the pump beam. An He–Ne laser at 633 nm used as the probe beam was inputted with an intensity of 1.0 mW/cm^2. The grating spacing could be controlled by changing the angle between the two beams. AFM view of the surface relief grating on the SGDR19 showed a depth of 15 nm and surface distance of 2.50 μm.

4. Conclusions

We synthesized successfully SGDR1, SGDR13 and SGDR19 containing azobenzene group by the condensation reaction between disperse red and ICPTEOS via the sol–gel process, which is confirmed by means of FT-IR and ^{1}H NMR. The diffraction efficiency of SGDR1, SGDR13 and SGDR19 film were observed up to a level of 0.65%, 0.24% and 0.99%, respectively. The SGDR-*n*s showed adequate writing–erasing–rewriting properties and a fairly stable diffraction level when used as a reversible optical storage material.

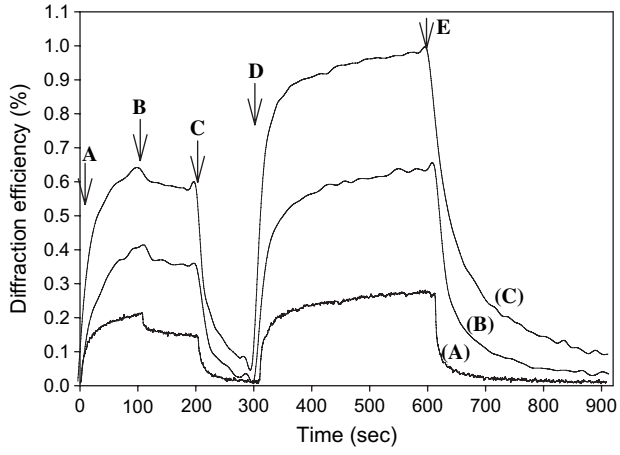

Fig. 6. Writing–erasing curve of SGDR1 (B), SGDR13 (A), and SGDR19 (C) film with an intensity of 25 mW/cm^2 (A, D: two beams turn on; B: two beams turn off; C, E: only one beam turns on).

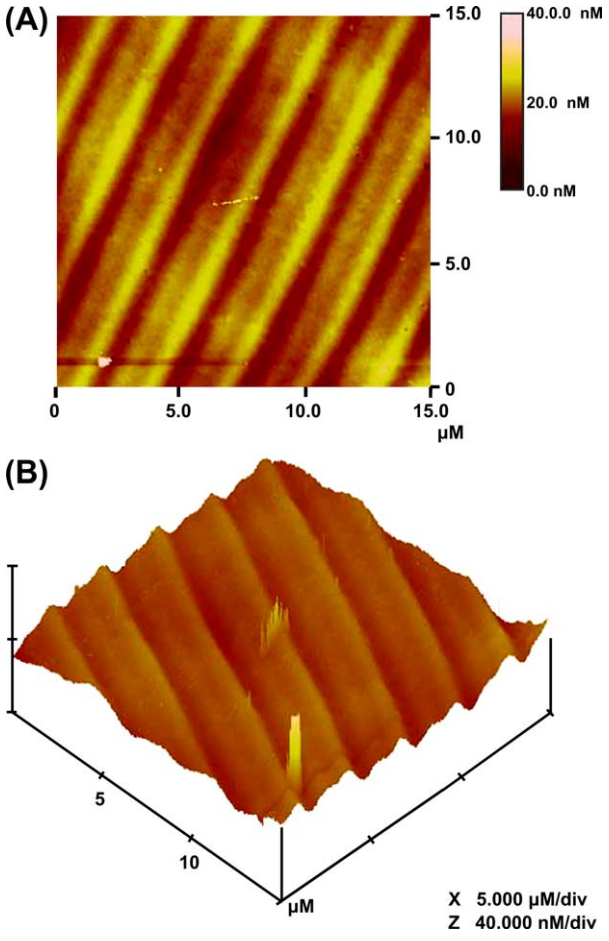

Fig. 7. 2D (A) and 3D (B) AFM views of the surface relief gratings on SGDR19 film.

Acknowlegement

This study was supported by the Basic Research Program of the Korea Science and Engineering Foundation through the Applied Rheology Center and Brain Korea 21.

References

[1] Luckemeyer T, Franke H. Appl Lett 1998;53:2017.
[2] Kumar G, Neckers DC. Chem Rev 1989;89:1915.
[3] Shi Y, Steier WH, Yu L, Chen M, Dalton R. Appl Phys Lett 1991;58:1131.
[4] Natanshon A, Rochon P, Gosselin J, Xie S. Macromolecules 1992;25:2268.
[5] Raschellá R, Marino IG, Lottici PP, Bersani D, Lorenzi A, Montenero A. Opt Mater 2004;25:419.

[6] Rosso V, Loicq J, Renotte Y, Lion Y. J Non-Cryst Solids 2004;342:140.
[7] Marino IG, Bersani D, Lottici PP. Opt Mater 2001;15:279.
[8] Muto S, Kubo T, Kurokawa Y, Suzuki K. Thin Solid Film 1998;322:233.
[9] Riehl D, Chaput F, Lévy Y, Boilot J-P, Kajzar F, Chollet P-A. Chem Phys Lett 1995;245:36.
[10] Chaput F, Riehl D, Lévy Y, Boilot J-P. Chem Mater 1993;5:589.
[11] Novak BM. Adv Mater 1993;5:422.
[12] Hopfield JJ, Onuchic JN, Beratan DN. Science 1988;241:817.